Genetic Algorithm in Tidal Range Schemes' Optimisation

Jingjing Xue*[1], Dr. Reza Ahmadian*[2], Prof. Owen Jones*[3]

Cardiff School of Engineering, Queen's Building,
The Parade, Cardiff, U.K. CF24 3AA

[1]XueJ7@cf.ac.uk

[2]AhmadianR@cf.ac.uk

Cardiff School of Mathematics
Cathays, Cardiff, U.K. CF24 4AG

[3]joneso18@cf.ac.uk

Corresponding Author:
Reza Ahmadian
e-mail: *AhmadianR@cf.ac.uk*

tel: (0044)7737581199

The total number of words of the manuscript, including entire text from title page to figure legends: **8443**

The number of words of the abstract: **200**

The number of figures: **8**

The number of tables: **3**

Genetic Algorithm in Tidal Range Schemes' Optimisation

Jingjing Xue[1], Dr. Reza Ahmadian[2], Prof. Owen Jones[3]

[1]XueJ7@cf.ac.uk
[2]AhmadianR@cf.ac.uk
[3]joneso18@cf.ac.uk

Abstract

Tidal energy has a significant advantage over many other forms of renewable energy because of the predictability of tides. Tidal Range Structures (TRSs) are one of the main forms of tidal renewable energy. Designing the operation of TRSs is one of the challenging aspects in early stages due to the large variety of scenarios. Traditionally this has been done using a grid search. However, grid search can be very elaborate and time consuming during the design of TRSs. This paper proposes a novel and more efficient method to optimise the design of the operation of TRSs by maximising their electricity generation using a Genetic Algorithm. This GA model is coupled with a 0-D model which breaks the tides into small units and considers flexible operation. This approach delivered more than a 10% increase in electricity generation when compared to non-flexible operation, i.e. using fixed heads for all tides, just by optimising the operation. The GA model was able to achieve the same amount of electricity compared to the best grid search method with flexible operation more efficiently, i.e. with about a 50% reduction in simulation time. The feasibility of the elite operational scheme is validated through a developed 2-D model.

Keywords: Tidal Energy; Tidal Lagoon; Genetic Algorithm; Optimisation of Operational Characteristics

1. Introduction

There is now a much better understanding of the impact of Green House Gasses (GHGs) on climate change and there is further social and political pressure to reduce GHGs [1, 2]. To achieve this, the development of renewable energy is more than necessary to meet current energy demand on a global scale [3]. Currently, 0.5 GW of commercial marine energy generation capacity is in operation and another 1.7 GW is under construction, with most of this accounted for tidal range [4]. As one of the new types of schemes, tidal lagoons are designed not to block estuaries or rivers and are considered to be more environmentally-friendly structures than other tidal structures including barrages, particularly due to having less impact on fish migration [5].

The main Tidal Range Schemes (TRSs) currently being considered in the UK are located around the Severn Estuary and Bristol Channel, in the South West of the UK [6], due to a mean tidal range of above 5 m which is often stated as required for a TRS to be cost effective [7, 8]. One such schemes is the 11.6 km^2 and 320 GW Swansea Bay Lagoon (SBL) [9]. SBL was granted planning permission by the UK Department of Energy and Climate Change (DECC) in June 2015 [10] and was positively supported by the independent Hendry Review, commissioned by the UK government and published in January 2017 [11]. However, the cost of electricity has been found to be an issue [12] and the UK government Business and Energy Secretary Greg Clark said that the £1.3bn project was not good value for money, despite claims to the contrary by the developers, Tidal Lagoon Power [13]. This further re-emphasises the importance of optimising TRSs to generate the maximum possible electricity and revenue while keeping cost down.

TRSs are designed to facilitate an artificial head difference through the operation of sluice gates and turbines and to use this head difference to generate electricity. Two of the key aspects of the operation of such schemes are the head difference when the scheme starts generating electricity and when generation stops. These have a significant influence on the basin water level and the discharge transferred across the impoundment, and therefore electricity generation. A fundamental theoretical study on the operation of TRSs was carried out by Prandle in the 1980s [14].

Prandle considered the head difference as a dimensionless parameter which was fixed throughout the operation simulation. Following that, fixed operating heads were implemented in several studies [15-18]. However, the fixed operation head schemes were sometimes found to result in the phenomenon of little or no power output during some neap cycles if the water head difference across the basin could not reach the prescribed starting or ending operation heads. It has been demonstrated that the electricity generation could potentially be improved by developing flexible operational heads [19, 20] without any extra cost. This increase in electricity generation could be up to 10% using local optimisation methods, such as gradient-based [21] and grid search methods [22]. However, a more advanced algorithm is essential to achieve global optimisation of TRSs due to the variability of tidal range over time and the fact that operation of each generation phase affects the water levels inside the basin which in turn impact the electricity generation of the next phase. Additionally, optimisation using local optimisation methods will require a large number of simulations of TRSs and could be very time consuming. This is more significant when various scenarios with different basin size and different number of sluice gates and turbines need to be considered during the design phase of the scheme. The choice of the design scenario influences the cost and annual electricity generation, i.e. revenue, and has a direct impact on the feasibility of the scheme and therefore it needs to be conducted to a high level of accuracy.

Evolutionary Algorithms (EAs) have been widely used as an efficient and time-effective optimisation tool which allows cutting-edge modelling especially in the fields of engineering and science [23]. EAs and particularly Genetic Algorithms (GAs), have been demonstrated to be a competitive method in the power market [24]. However, the application of GAs to marine renewable energy has been limited [25-28]. Leite Neto et al. [28] and Sullivan et al. [25] investigated the potential of using GAs for the optimisation of dispatch and arrangement of tidal turbines, respectively. Their work demonstrated the ability of GAs to find a successful number and arrangement of tidal stream turbines, with maximum electricity generation, minimum cost and appropriate performance. Furthermore, Child and Venugopal showed that superior results can be obtained using GAs for the optimisation of wave energy converters layout [26]. Their results were consistent with the findings of Kontoleontos et al. which proved that it was possible to predict tidal stream energy using EAs with a satisfactory result [27]. However, there was no study found in the literature using GAs or similar EAs to optimise the flexible operation scenarios of the tidal range structures.

This paper mainly focuses on facilitating the development of TRSs by using an improved GA model to optimise them. The study includes splitting the operation into the smallest generation components, i.e. half of the duration of a tide. The GA model was developed using a 0-D model as the fitness assessment and with different recombination methods. The prediction of electricity generation using the GA model was compared with the most promising approach for grid search reported by Xue et al. [22] as benchmarks, namely Every Half-tide and Next (EHN). The GA model achieved the same amount of electricity but more efficiently. The optimised operation schemes were then implemented in a more sophisticated 2-D unstructured model, namely the Depth Integrated Velocities And Solute Transport (DIVAST 2-DU) model, in order to validate the applicability of the operation schemes derived by the GA model which uses the 0-D model. The predicted electricity among various scenarios were compared which approved the reliability of application of the GA model in optimisation of operation of TRSs.

2. Genetic Algorithm

The idea of the GA was inspired by simulating the Darwinian evolutionary processes which are naturally occurring in chromosomes [29]. It was first introduced by John Holland in the early 1970s [30]. The method is iterative and each iteration, called a generation, is expected to produce better solutions. Each solution is comprised of a number of parameters and is called an individual or a chromosome. Each of the parameters being optimised is called a gene. A collection of individuals considered at each iteration to find the most optimised individual is called a population. For each generation, suitability of all individuals (or solutions) are evaluated based on a fitness function. Moreover, the term fitness function was also replaced by fitness assessment in order to clarify this further. The implementation of

the GA model finishes when the predefined termination criterion is satisfied for an individual or the predefined maximum number of iterations has been reached. If the termination criterion is not met, iteration continues and a new generation is produced using the fitness information in combination with three different processes, namely mutation, recombination and selection [29, 31]. Contribution of each of these processes in production of the new generation is set using a predefined statistical parameter.

Mutation is a genetic operator used to maintain genetic diversity from one generation of a population to the next. The purpose of the mutation is to overcome local optima and to exploit new regions of the searched space. The probability of mutation, namely P_m shows the likelihood of mutation on an individual. The mutation step typically operates on a randomly chosen gene or genes on chromosomes which are randomly selected from parents. The model uses the Sequential Mutation Method (SMM) to implement mutation. More-recent studies have shown that SMM, which applied mutation to only one gene in each chromosome while the other genes survive, could speed up the process. This is due to the reduced number of calls to the cost function which in turn increases the efficiency of GAs [32]. In the SMM, the selection of the only gene which changes is carried out sequentially, and as shown in Figure 3, the selected genes move one step further as the number of generations increases.

Recombination generate a new individual by combining the genes from two randomly-selected individuals using probability of recombination, namely P_r, which represents the likelihood of mixing of attributes from different chromosomes [31]. P_r is recognized as one of the distinguishing features of GAs [30, 33]. Two main approaches for recombination in GAs are the Linear Recombination Methods (LRM) and the Ring Recombination Methods (RRM). The former considers a linear representation of each individual and sections of two individual, also called parents, are recombined to generate the individuals in the next generation as shown in Figure 4 [34]. The RRM is based on the fact that polyoma DNA molecules exist in cyclic forms of equal molecular weight as well as linear form [35, 36] and such cyclic DNA forms display more diversity in the offspring. It has been found that using RRM with SMM could enhance the convergence of GAs in comparison with using LRM by reducing the number of times that the fitness assessment has to be called [32]. This model uses RRM with SMM and further discussion on this is given in Section 5.2 [32].

The probability of selection, namely P_s, is used to control 'the fittest survival' or the selection of the best solutions for the next generation. It is generally set to 1 which means that all better solutions are selected for production of the next generation following the calculation of the fitness of each individual in the generation. As a result, it is expected that 'the weak' solutions are abandoned [31].

In GA approach, a small number of the 'elite' organisms may pass unchanged to the next generation [37], which results in inclusion of the better members of the previous generation in the new generations. The families of elites will be expanded and come to dominate their populations over successive generations, while the disadvantaged groups will be eliminated through the selection process [25].

GA computational model can be parallelized to exploit the capabilities of high-performance computers and distributed systems, ensuring the efficiency of the GA models [38, 39]. Hence, parallelization of calculation of fitness, e.g. the electricity generation as described in Section 4.1, would be more efficient if there is a good match between the number of initial solutions and the number of processors available.

As mentioned in Section 1, GA models have been widely applied in various fields of engineering and science and there are several existing GA software. However, problem-specific GA modelling, as used in this study, is still commonly used due to its flexibility in definition of the problem and efficiency of the GA model [25, 40].

3. Tidal Range Schemes

3.1. Operation

There are three main generation modes, namely flood-only , ebb-only and two-way generation, in which the ebb-only and two-way generation modes are considered as the two most effective operation schemes [17]. Figure 1(a) and 1(b) are schematic illustrations of these operation schemes.

For ebb-only generation and starting at a high tide, the holding stage commences when water levels outside and inside of the impoundment are almost the same. Holding at high water ends and the ebb-generation phase starts when the head difference across the impoundment reaches a pre-set starting generation head value, referred to as H_s herein. At this stage, only turbines are opened and the head difference across the impoundment is used to generate electricity efficiently. This phase then continues until the head difference across the impoundment embankment is smaller than an assumed ending head, referred to as H_e herein. The second holding phase starts again with both turbines and sluice gates closing. As flood tide starts and water levels outside the impoundment become higher than the inside, the filling phase starts by opening both sluice gates and turbines, without electricity generation, to allow the impoundment to fill. The next cycle starts again with the holding phase at high water when the water levels inside and outside of the impoundment are close. A schematic of the ebb-only generation scheme is illustrated in Figure 1(a).

Similarly, the two-way generation holding phase at high water starts when the water levels across the impoundment are close. Ebb generation commences when the head difference reaches a designed starting head for ebb tides, namely H_s, by operating the turbines. This stage is finished when the head difference across the impoundment is no longer enough to generate electricity or it is less than the ending head, H_e, for ebb generation. The filling phase starts at this stage which allows more water to flow out of the basin by opening both sluice gates and turbines until the water levels across the impoundment are the same. The flood holding stage continues until the head difference across the impoundment reaches the starting head again but for flood generation, referred by the second H_s in Figure 1(b). At this stage the turbines are allowed to operate and a second phase of electricity generation or a flood generation phase starts. When the head difference across the structure is smaller than the ending head again but for flood generation, known as the second H_e in Figure 1(b), a flood filling phase commences with both sluices gates and turbines opening which raises the water level inside the impoundment. The holding phase at high water starts again once almost the same water level is achieved between the inside and outside of the impoundment. This can be seen as a periodic process, which is repeated during each cycle. A schematic of the two-way generation scheme is illustrated in Figure 1(b).

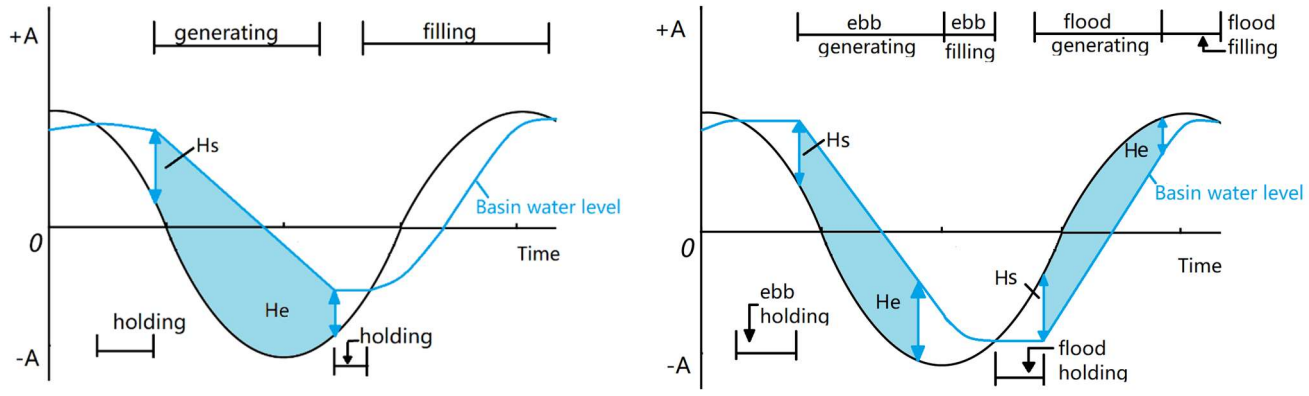

Fig. 1. Schematic representation of the operational schemes: (a) one-way ebb-generation; (b) a two-way tidal power plant.

3.2. Swansea Bay Lagoon

Swansea Bay is located in the South West of the United Kingdom and constitutes part of the South Wales coastline. As a part of the Bristol Channel, the tidal range in the bay could rise to about 10 m [41], which makes it a suitable location for a tidal range scheme. Swansea Bay Lagoon (SBL) has been proposed to be built with a 9.5 km-long wall

encompassed in Swansea Bay. The scheme would consist of 16 bulb turbines, each with a diameter of 7.2 m, and with an installed capacity of 320 MW [10]. The scheme would generates approximately 530 GWh per year [42] with an installed capacity of 320 MW and a two-way generation mode, corresponding to a capacity factor of about 18.9% on average , and the area of the sluice gates would be approximately 800 m^2 [41, 43]. The UK Government has decided not to support the scheme yet due to the high cost of electricity [44].

4. Modelling Methodology

4.1. 0-D modelling

4.1.1. 0-D model setup

In 0-D modelling, the basin water levels are calculated from the previous upstream and downstream water levels according to the continuity principle. The model assumes that the water is distributed uniformly and instantaneously in the impoundment when the inflow or outflow go through turbines and/or sluice gates, instead of using a more complex but realistic 2-D modelling approach. One commonly-used technique is the backward-difference numerical model, developed according to the continuity equation. Water levels outside the basin are driven by tides. The upstream and downstream water levels at a particular time, e.g. the i^{th} time step, are Z_{up}^{i} and Z_{dn}^{i}, respectively. The upstream water level at the next time step of i+1, namely Z_{up}^{i+1}, can be calculated as follows:

$$Z_{up}^{i+1} = Z_{up}^{i} + \frac{Q(H)+Q_{in}}{A(t)}\Delta t \quad (1)$$

where Q_{in} is the inflow/outflow to the lagoon through sources other than through the TRS, e.g. a river or outflows; $A(t)$ is the wetted plan surface area of the lagoon at the time t and $Q(H)$ is the total discharge through the turbines and sluices which will be discussed further in Section 4.1.2 [45].

Tidal data generated from the DIVAST 2-DU model, of Swansea Bay in its existing condition was used to provide the downstream water levels for the 0-D model. The 0-D model was first set up with conditions reported by Petley and Aggidis [41], namely 3.0 m of H_s and 1.0 m of H_e, to validate the model. The annual energy generated was predicted to be 472.89 GWh which is within 2% of the value reported by Petley and Aggidis [41]. This is considered to be acceptable and the very limited difference could be due to differences in the downstream water levels or details in operation of the lagoon.

Year 2012 was chosen for this study due to the availability of a complete set of boundary conditions and availability of validation data for the 2-D model. Details of power output over 2012 and its variation per tidal cycles were shown by Xue et al. [22]. It showed that the 2nd cycle of the year, which was from 421.5 hr to 782.80 hr from the start of 2012 had an average power output very similar to the annual power output. Since optimising the operation for every half-tide for the duration of a year was very computationally expensive, this typical spring-neap tidal cycle, i.e. the 2nd cycle of the year, was used for optimisation.

4.1.2. Energy and discharge calculation

The discharge through a turbine and electricity generation was calculated based on head difference across the structure using a hill chart as shown by Petley and Aggidis [41]. The flow through a sluice gate (Q) was obtained using the orifice equation as follows [46, 47]:

$$Q = C_d A_s \sqrt{2gH} \quad (2)$$

where C_d is the discharge coefficient; g is gravitational acceleration (m/s^2); A_s is the sluice gate area (m^2) and H $=Z_{up} - Z_{dn}$.

4.2. 2-D modelling

4.2.1. Governing equations

The DIVAST 2-DU model which solves the depth-integrated 2-D Reynolds average equations for incompressible, unsteady and turbulent flows [48] has been used in this study. The model has been widely used to investigate the hydrodynamics, power output prediction and sediment transport [15, 49]. The domain decomposition technique [17, 50] has been used to simulate TRSs in this study. In this method, the domain of study is divided by the structure into inside and outside sub-domains. The subdomains are fully detached but dynamically linked through internal boundaries which are governed by the discharges through turbines and sluice gates [17, 46]. The model has been refined to operate flexibly [22] and the operations of the turbines and sluice gates were coupled with a ramp sinusoidal function for opening and closing to provide a smooth operation [50].

The 2-D depth integrated mass conservation and momentum conservation equations in x and y directions are given in Eqs. 4-5, respectively. The momentum equations include the effects of bottom friction, wind shear, the earth's rotation and turbulence [51].

$$\frac{\partial \xi}{\partial t} + \frac{\partial q_x}{\partial x} + \frac{\partial q_y}{\partial y} = 0 \tag{3}$$

$$\frac{\partial q_x}{\partial t} + \beta\left[\frac{\partial u_x}{\partial x} + \frac{\partial v q_x}{\partial y}\right] = f q_y - gH\frac{\partial \xi}{\partial x} + \frac{\tau_{xw}}{\rho} - \frac{\tau_{xb}}{\rho} + \varepsilon\left[2\frac{\partial^2 q_x}{\partial x^2} + \frac{\partial^2 q_x}{\partial y^2} + \frac{\partial^2 q_y}{\partial x\,\partial y}\right] \tag{4}$$

$$\frac{\partial q_y}{\partial t} + \beta\left[\frac{\partial u q_y}{\partial x} + \frac{\partial v_y}{\partial y}\right] = f q_x - gH\frac{\partial \xi}{\partial y} + \frac{\tau_{yw}}{\rho} - \frac{\tau_{yb}}{\rho} + \varepsilon\left[\frac{\partial^2 q_x}{\partial x^2} + 2\frac{\partial^2 q_x}{\partial y^2} + \frac{\partial^2 q_x}{\partial x\,\partial y}\right] \tag{5}$$

where ξ is the water surface elevation above datum (m) and q_x, q_y are the discharges per unit of width in the x and y direction, respectively (m^2 s^{-1}); β is the momentum correction factor for non-uniform vertical velocity profile; f is the Coriolis parameter, which is caused by earth rotation (rad s^{-1}) and g is the gravitational acceleration (m s^{-2}); τ_{xw} and τ_{yw} are the components of the surface wind stress in the x- and y-axis directions respectively (N m^{-2}); τ_{xb} and τ_{yb} are the bed shear stress in the x and y directions , respectively; and ε is the depth-averaged eddy viscosity (m^2 s^{-1}). The DIVAST 2-DU model was modified to simulate the electricity generation and performance of TRSs based on a flexible operation scheme. Further details about the 2D model and implementation of TRSs in the model can be found in [16, 17].

4.2.2. Model validation

The Bristol Chanel and Severn Estuary including the proposed SBL were simulated using the DIVAST 2-DU model. The model covered an area of 5,805 km^2 and the bathymetry data interpolated at the nodes from EDINA Digimap [52]. This bathymetry was modified to match the proposed depth of the dredging channels which encloses the turbines houses [53]. The seaward boundaries were obtained from the National Oceanographic Centre [19], covering the simulation period. The water levels and currents predicted by the model without the lagoon were validated against field data including ADCP data, including three points representing the Western, Central, and Eastern parts of the Bay, namely L2, L3, and L5 as shown in Table 1. A comprehensive validation including hydrodynamics of the 2-D model was carried out in this study to demonstrate the reliability of the simulation, although the water level is the most significant factor to influence the energy output rather than the currents and their directions. The comparison of measured and predicted water levels, current velocity and directions can be found in [22]. The root mean square error (RMSE) and the R-squared (R^2) of differences between the predicted and measured water levels and current speeds at all three validation sites are included in Table 1. It indicates good correlation between the

predicted and measured values with errors in the predicted water levels being less than 0.15 m. Hence, it can be concluded that the model agrees well with the observed data and, therefore, can be reliably used to model the key hydrodynamic parameters of elevations and velocities over the domain of interest. The average elements length varies from 50 m in the proximity of the lagoon up to 1,200m close to the seaward boundary. Further details of the 2-D model can be found in Xue et al. [22].

Table 1. Analysis of measured and predicted data at L2, L3, and L5.

No	Location	Latitude	Longitude	Terms	RMSE	R^2
1	L2	51°31.78′ N	003°58.96′ W	Water Level (m)	0.111	0.997
				Velocity (m/s)	0.055	0.832
2	L3	51°33.56′ N	003°56.32′ W	Water Level (m)	0.136	0.997
				Velocity (m/s)	0.031	0.774
3	L5	51°31.82′ N	003°51.25′ W	Water Level (m)	0.147	0.997
				Velocity (m/s)	0.017	0.787

5. Operational Optimisation of Swansea Bay Lagoon

The main aim of the GA model developed in this study is to identify an operation schemes which will result in maximum generated electricity. The performance of the GA model was assessed by comparing the predicted electricity generated using this model and a traditional grid search model. The grid search model used was based on the Every Half-tidal cycle and Next (EHN) approach which was the typical and most promising approaches in the optimisation of the operation of TRSs [22].

5.1. Optimisation with the EHN approach

In this study, every operational scheme is encoded as two vectors, namely $[H_{s,n}]$ and $[H_{e,n}]$, representing the operation water heads for n successive tides: that is $[H_{s,1}, H_{s,2}, \dots, H_{s,n}]$ for starting heads and $[H_{e,1}, H_{e,2}, \dots, H_{e,n}]$ for ending heads of half-tides as shown in Figure 2. The ranges of starting heads for ebb and flood tides, i.e. $H_{s,1}$ for the half-tide A, were from 2.0 m to 8.0 m with 10 cm increments. Meanwhile, ending heads for ebb and flood tides, i.e. $H_{e,1}$ for the half-tide A, were covering a range from 0.5 m to 4.5 m, also with an increment of 10 cm. This resulted in 5,760 million scenarios for each pair of half-tides ($60 \times 40 \times 60 \times 40$ where the 1st and 3rd numbers were for H_s of 1st and 2nd half-tides, respectively, and the 2nd and 4th numbers were related to H_e of the 1st and 2nd half-tides, respectively) or about 8.1 billion scenarios for one year of operation to consider in this case. This will result in a very large number of scenarios during the design of the operation schemes where various numbers of turbines and sluice gates are being considered. The EHN model was run with a time step of 1 minute. An average spring-neap tidal cycle, over 14 days, was selected as the simulation period. Similarly to previous study by Xue et al. [22], the simulation period for this case was the 2nd cycle in the year of 2012, as mentioned in Section 4.1.1.

Figure 2 shows two synthetic tides to demonstrate EHN approaches. In the EHN approach, optimisation is carried out for every generation phase which occurs over a half-tide as shown in Figure 2. For example in this figure, ebb and flood half-tides correspond to half-tides A and B, respectively. However, since the water level inside the impoundment at the end of each operation cycle will be the starting water level in the next operation period, maximising electricity output for one operation period phase irrespective of next period could jeopardise the electricity generation of the next period. Therefore, in this method the next half-tide was considered in selecting the most-optimised generation for each operation period. For each half-tide, a range of operational heads are considered and generated electricity over that half-tide and the next one is calculated. This starting water level inside the basin is the ending water level of the last

half-tide with the maximum generated electricity. For example, to find the best operational heads for half-tide B in Figure 2 which corresponds with the second operation step, generated electricity of both half-tides B and C will be calculated using the water level inside the impoundment from the best operation of half-tide A. The operational heads generating the maximum electricity for both of the half-tides, B and C in this example, will be selected as the elite operation for half-tide B. The next step will be searching for the optimum operational heads of the next half-tide, i.e. C in this example, starting with the water level of the optimum operation of half-tide B for inside the basin. This way, the link between operation cycles is considered and the operation of each cycle can be influenced by not only generated electricity in that cycle but also the next cycle. This link is achieved at extra computational cost.

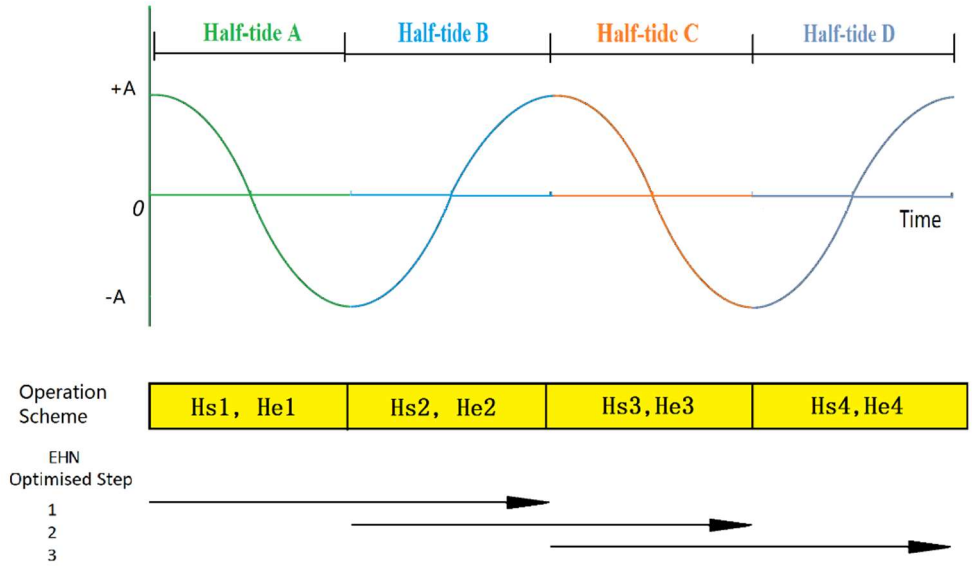

Fig.2. Schematic illustration of EHN optimisation methodology [22].

Maximum electricity generated using the EHN model for the simulation period is shown in Table 2. The EHN model flexible head operation has shown a more than 10% improvement in electricity generation, in comparison to the fixed head operation. The maximum electricity over the simulation period for a fixed-head operation schedule, known as the non-flexible operation schedule, was achieved with a starting head of 4.6 m and an ending head of 1.9 m [22].

Table 2. Comparison of different approaches used to optimise the operation of TRSs.

Optimisation methodology	Energy over 1 tidal cycle (GWh)		Change to energy prediction using 2-D with fixed head operation (%)	Difference between 2-D and 0-D energy prediction (%)
	0-D model	2-D model		
Grid Search fixed head operation	21.3	19.7	-	-7.5%
GA model	24.0	23.0	16.0%	-4.6%
Grid Search EHN model	24.0	22.9	16.0%	-4.6%

5.2. Optimisation using the GA

The pseudocode of the GA model is listed in Table 3 and the steps in executing the GA model can be summarized as follows:

I. Randomly create a certain number of solutions with flexible operational characteristics for every half-tide in the selected typical cycle.
II. Iteratively perform the following sub-steps on every population until the termination criterion has been satisfied:
    i. Copy existing individual solutions to the new solutions with their specific energy outputs.
    ii. Create new solutions from the copied solutions by randomly mutating the operational heads at each half-tide in every scheme.
    iii. Create new solutions by genetically recombining sub-solutions which are randomly chosen from all solutions, including mutated solutions and non-mutated solutions.
    iv. Evaluate the energy generation of the solutions over all the selected typical cycle, based on the principle of 'survival of the fittest'.
III. The best operational scheme with maximum electricity generation that appeared in any generation (i.e., the best so-far scheme) is designated as the optimised result of the GA for the run. This result may present a scheme (or an approximate scheme) to the operational characteristics optimisation.

Table 3. Pseudocode of the Genetic Algorithm.

Algorithm The pseudocode of the GA
proc Set_up //Set up algorithms parameters
Generate the initial operation schemes and evaluate their fitness;
While NOT **Termination_criterion**() do
Offspring <- **Copy**(Parents);
Offspring <- **Mutation**(P_m, Offspring);
Offspring <- **Recombination**(P_r, Offspring);
Evaluate_Fitness (Offspring);
Survivals <- **Selection**(P_s, Parents, Offspring);
Parents <- Survivals;
End While
End Proc Set_up;

In the GA, an operation scheme including the starting and ending heads for every half-tide was considered as an individual with different genes. The GA method uses a population of solutions/individual which are updated iteratively. Each iteration of solutions was also referred to as a generation in the GA model and therefore the n^{th} iteration was referred to as the n^{th} generation. In every iteration, a new population was generated based on the most optimum solution of its previous population through the mutation, recombination and selection. The new populations were referred to as offspring in the GA while the previous population was referred to as the community of parents. To control the population size during each generation, the best genes were selected based on their performance using a fitness assessment, i.e. the electricity generation predicted over the simulation period, calculated using the 0-D model in Section 4.1; that is, the electricity generation of parents and offspring during each iteration was evaluated. Then the solutions with higher electricity generation were selected to survive and were considered as the parents for its following iteration. This process was referred to as selection, which was designed with the intention of imitating the process of natural selection and evolution.

The GA model was developed as a part of this study using the Sequential Mutation Method (SMM), Linear Recombination Methods (LRM) and Ring Recombination Methods (RRM). In SMM, only one half-tide, e.g. half-tide i within the successive half-tide n, could be selected for mutation and the selection of the half-tide follows a sequence with the generation increasing, that is, the half-tide(i+1) would be selected for mutation in the next generation, as shown in Figure 3. In the selected half-tide i, the operation heads of $[H_{s,i}]$ and $[H_{e,i}]$ could be mutated with the

probability of P_m as mentioned in Section 2. The mutated operation head follows a normal distribution with an assumed variance of 0.1 herein and a mean of this distribution of the initial operation head during its generation. That is, the change of mutated operation head was according to the operation head before mutation. This representation gave insight into the nature of evolution that the genes' mutation of children kept a certain relationship with the genes from their parents, so that it is possible to find the optimum range of change within the search space that resulted in greatest improvement. If the number of the generation reaches half-tide n, in the (n+1) generation, the mutation will be applied on the 1st half-tide and this process is continued. Although the SMM in the mutation process was supposed to improve the original algorithm efficiency, it still suffered from being slow especially when the size of initial population was extremely large.

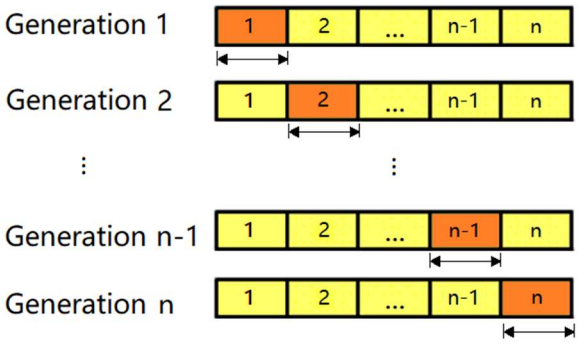

Fig.3. Sequential Mutation Methods (SMM) illustration (the highlighted cell represents the place of applying the mutation in each generation).

Moreover, it is believed that the recombination does enhance the performance of GAs [31]. In both of the yellow and blue bars representing the selected solutions in LRM as shown in Figure 4(a) and as described in Section 2, the bits in the two points are swapped between the 'parent organisms' [31] as shown in Figure 4(b). This strategy can be generalised to n-point crossover from any positive integer i, picking L crossover points randomly. However, as illustrated in Section 2, the RRM was able to further develop the GA model by imaging operational heads in every scheme was a circle, as shown in Figure 5(a) and (b). Similarly to LRM, two solutions were selected for recombination in Figure 5(a), then the recombined solutions were generated after exchanging information as shown in Figure 5(b).

Parallelization was one of the appealing features of this GA model, which was achieved by utilising the Open Multi-Processing (OpenMP) and 10 CPU with a High-Performance Computer (HPC) for approximately 1,640 minutes. As the cost time of energy calculation for each scheme was the same within a certain period, so the evaluations of a number of possible solutions could be represented at the same time and hence no consideration was needed to be given to the inevitable variation of cost time within every single generation.

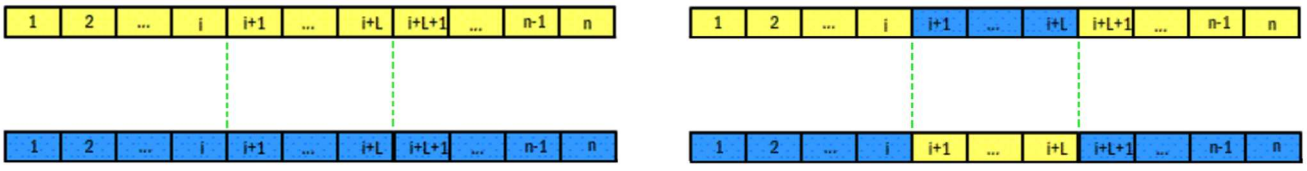

(a) (b)

Fig.4. Linear Recombination Methods (LRM) illustration: a) before LRM; and b) after LRM.

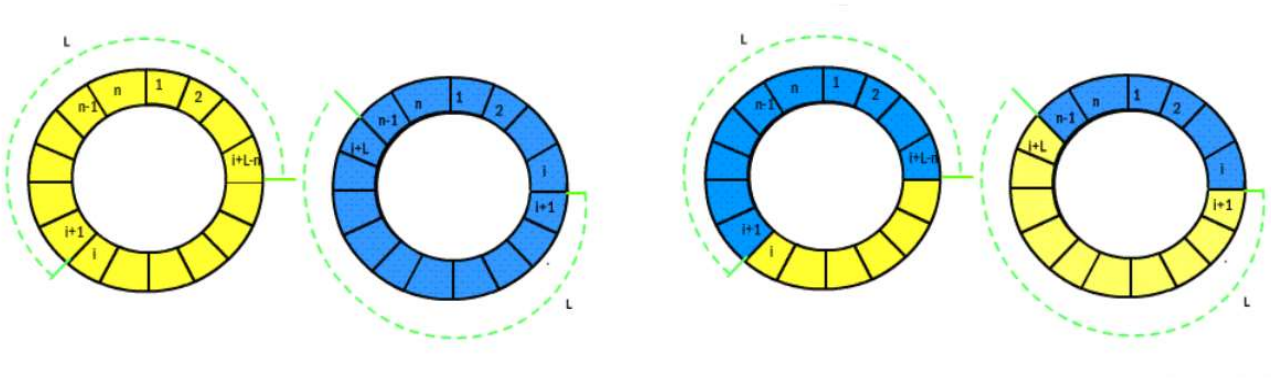

(a) (b)

Fig.5. Ring Recombination Methods (RRM) illustration: a) before RRM; and b) after RRM.

It has been shown that the efficiency of GAs highly depends on their parameters settings [54]. Furthermore, the optimisation could be completed faster with appropriate parameters [31]. In this study, P_m, P_r and P_s were assumed to be 0.5, 0.5 and 1, respectively, based on the literature [55]. This was assumed to be satisfactory for this research as the desired performance was achieved by the GA model. However, the impact of the choice of parameters used in the simulation and their influence on the performance of the GA model will be studied in future work.

In order to obtain optimised results while avoiding an endless running of this GA model, two termination criterions were defined herein. That is, if the energy production of the most elite scheme for the generation reached the ideal generated energy which was given by users, or the maximum number of generations or iterations was reached, then the GA process was ended and the optimisation results were output. It should be noted that in this case, the ideal generated electricity was set to infinity as the more energy generation obtained the better. The number of iteration was set to 3000, ensuring a sufficient time to achieve convergence. As the most important factor affecting the running time of the GA model, the size of initial solutions was supposed to be 1000, considering that more initial solutions generated means more time spent in energy output calculation and so is more time-consuming. While a large solutions size provided more individuals for testing, it also diluted the fitness of the best scheme [31]. In this study, the GA model was operated in the selected 2nd cycle with a time step of 1 minute, the same as in Section 5.1, allowing the reliability of the comparison between the GA and EHN models which would be discussed further in this section.

The GA model was run a number of times and it was found that the performance of the model is consistent. A typical comparison of power output over the typical tidal cycle during 3,000 iterations using LRM and RRM methods is shown in Figure 6. The GA model using RRM was converged after approximately 1000 iterations while LRM converged after 1500 iterations and hence RRM was roughly 30% less computationally expensive compared to LRM. Moreover, as an advanced approach to finding elite solutions, RRM was able to yield approximately 24.0 GWh of energy over the typical tidal cycle instead of 22.8 GWh when LRM was utilised. Higher efficiency and superior performance of RRM has been consistent with the findings of Nia and Alipouri [32] and therefore RRM has been used in the GA model developed in this study.

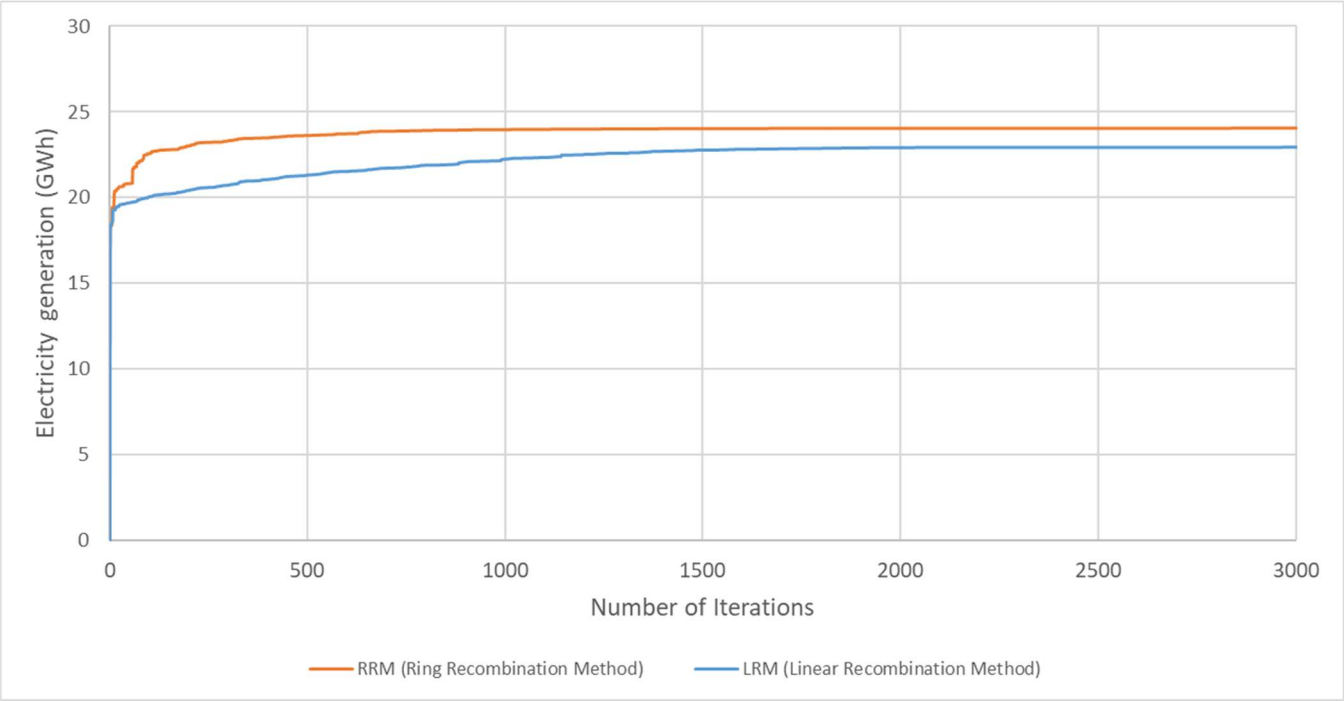

Fig.6. Convergence speed comparison.

The energy output of operation schemes optimised by different methodologies has been summarised in Table 2. It shows that using the GA model, which used half-tides' starting and ending heads as genes, had improved energy output by 16% compared to the grid search method with fixed operation heads. The GA model could perform as well as the best-performing grid search model, i.e. the EHN model, while GA model simulation time has been 50% lower than the EHN model.

Figure 7 illustrates the comparison of the lagoon operation optimised by GA and EHN models for a tidal cycle, in terms of the (a) water levels and optimum operation heads, (b) energy output and (c) operation scheduling. It illustrated that there are only negligible differences between the GA and EHN models for optimised operational characteristics, including operation of the scheme and therefore generated electricity and water levels, but with at least 50% computational time saved by using GA. Consequently, GA is able to reach the same performance as EHN but with higher efficiency.

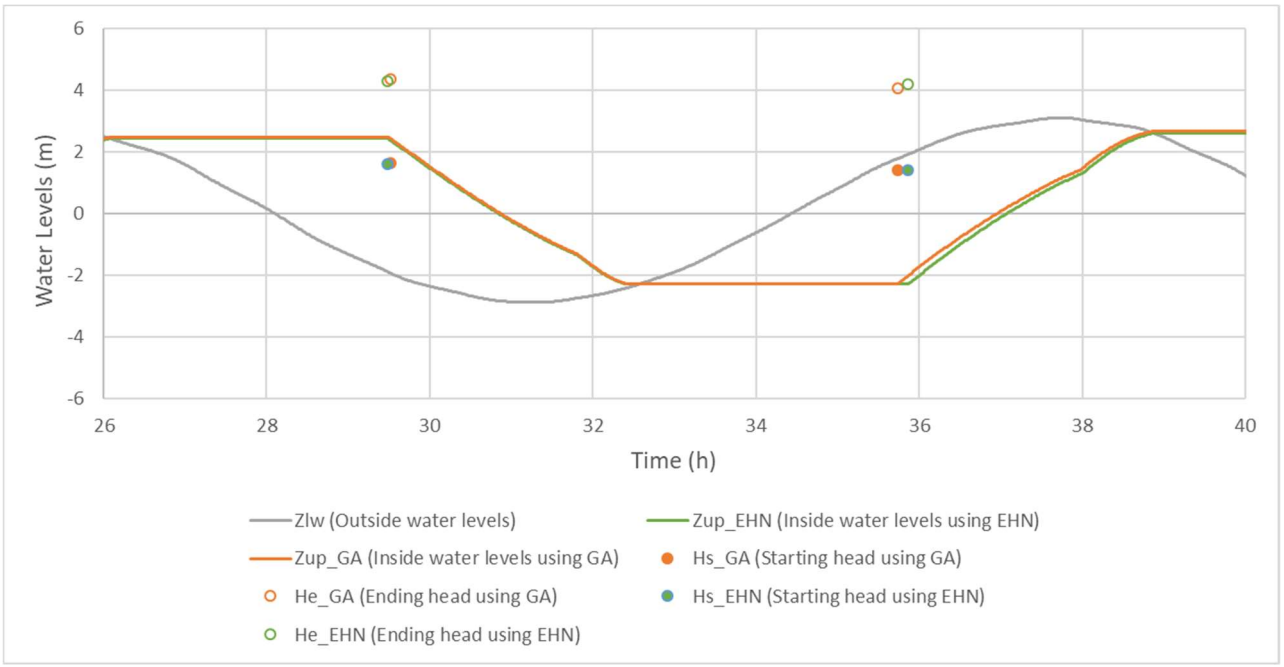

(a)

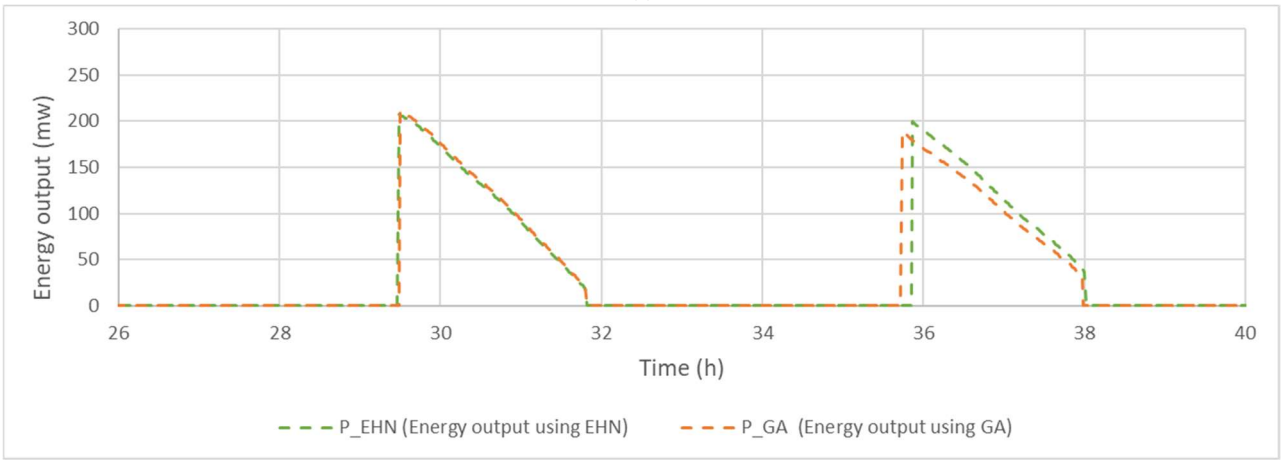

(b)

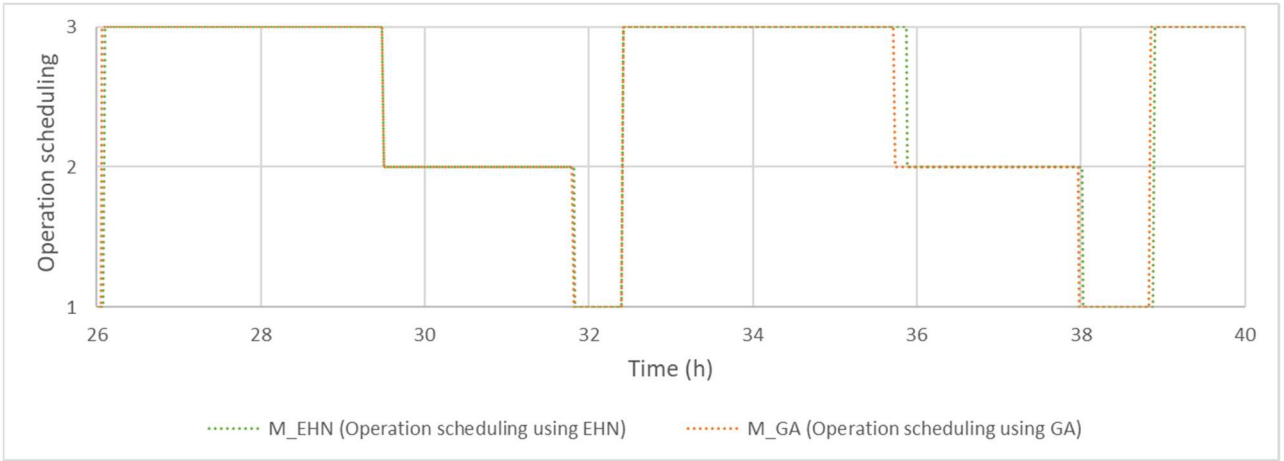

(c)

Fig.7. The comparison of the lagoon operation optimised by GA and EHN models for a tidal cycle, between a) water level and optimum operation heads; b) energy output and c) operation scheduling, in which 1-3 represents filling, generating and holding, respectively.

5.3. Comparison between 2-D and 0-D models

In order to validate the performance of the GA model which used a 0-D model as the fitness assessment, the DIVAST 2-DU model was implemented to simulate the SBL and then its electricity generation was evaluated using the solution obtained from the GA model. The comparison of output predicted by 0-D and 2-D models is shown in Table 2. It can be seen that the difference between 2-D and 0-D models is lower than 5% when utilising the flexible operations. It should be mentioned that the electricity prediction in 2-D could be influenced by various sources of uncertainties including storm surges although the effect was proved to be relatively limited [7].

Figure 8 (a)-(c) shows the difference between the performance of the lagoon predicted by the 0-D and 2-D models using the operation scheme optimised by the GA model. It illustrates the proximity and therefore applicability of the 0-D model to more accurate 2-D predictions while used for optimising of the operation of TRSs as a part of the GA models.

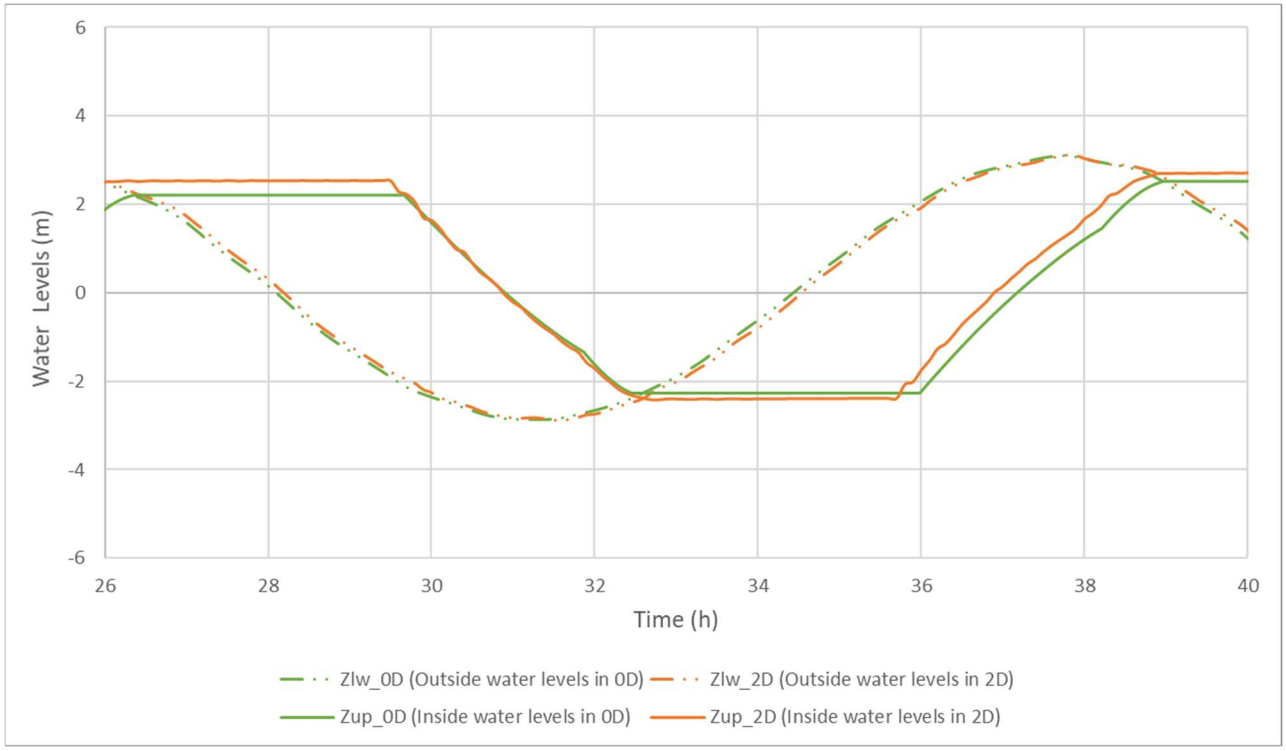

(a)

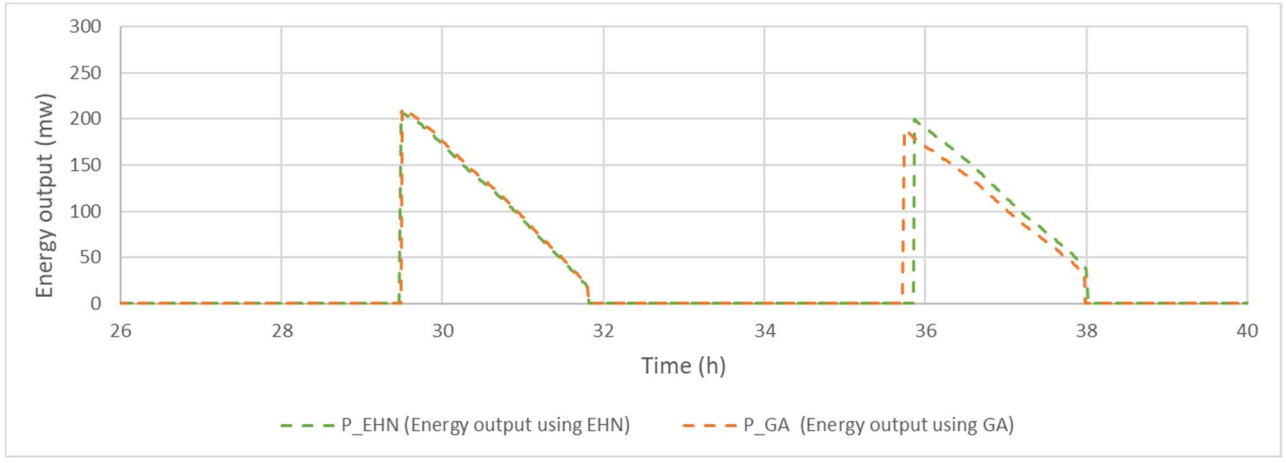

(b)

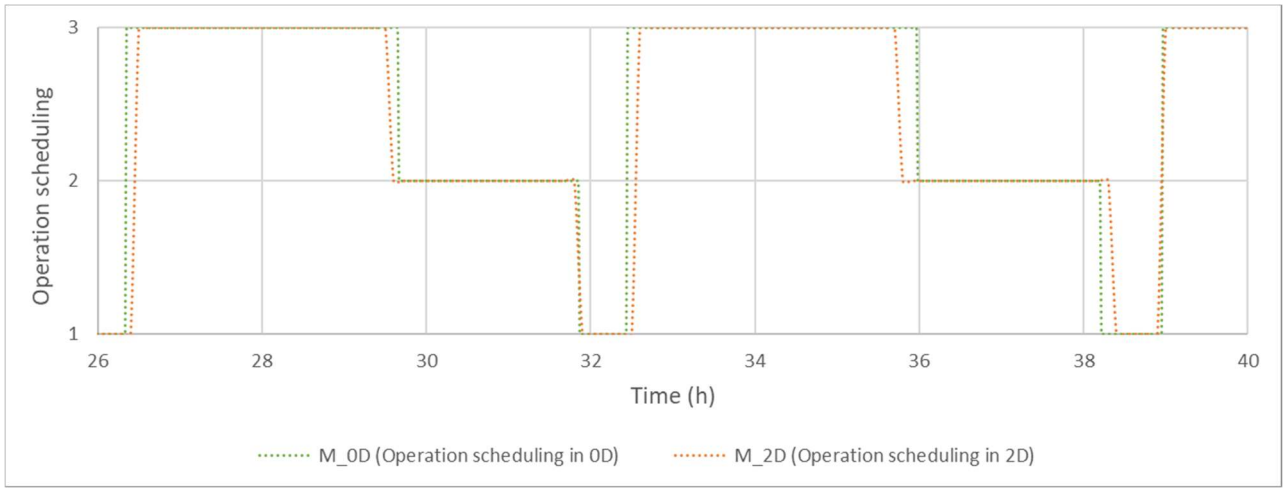

(c)

Fig.8. The comparison of the predicted performance of the lagoon in 0D and 2D using the operation optimised by the GA model for a tidal cycle, between: a) water levels inside and outside the lagoon; b) energy output and c) operation scheduling, in which 1-3 represents filling, generating and holding, respectively.

6. Conclusions

The study presented here has demonstrated the application of a GA in optimising the operation of TRSs using a case study of the proposed Swansea Bay Lagoon (SBL). In the GA model, prediction of generated electricity has been achieved by implementing the 0-D model method as the fitness assessment. Along with the increase of generations, operation heads in every scheme were required to reproduce through the mutation, recombination and selection. A mutation method used was Sequential Mutation Method (SMM). Linear Recombination Methods (LRM) and the Ring Recombination Methods (RRM) were implemented as recombination methods, to compare the optimisation performance and convergence speed of the GA model. The prediction of the electricity generation using the GA model was compared with the traditional fixed operation and the best performing grid search model reported by Xue et al. [22], namely the Every Half tide and Next (EHN) model.

The results showed that the GA model could improve the operation of the scheme and generate more than 16% of energy over the simulation period when compared with a fixed-head grid search model. However, the GA model showed the same outcomes as the most optimised grid search model, namely the EHN model, while the simulation time of the developed GA model was reduced by at least 50% compared to the simulation time of the EHN model. It demonstrated the capability and potential of using GA to improve the outcomes of TRSs optimisation with higher efficiency, especially when a large number of scenarios with different basin size, different number of sluice gates and turbines are required to be considered during the design phase of a scheme or simulation of multiple schemes. The more efficient GA model could also be used in real-time modification of the operation of TRSs in response to the grid requirements. This could influence the cost and annual electricity generation, i.e. revenue, and so has direct impact on the feasibility of TRSs.

Finally, the operation schemes which have been optimised by the fixed head and EHN grid search models as well as the GA model have been implemented in a more sophisticated 2-D model, and the differences between the 0-D and 2-D models were highlighted. The energy output predicted by the 2-D model using the flexible operation generated from the GA model has been within the 5% of the energy output predicted by the 0-D model. This level of error is consistent with the predicted electricity difference between the 0-D and 2-D models using operation schemes designed by the EHN grid search model [22]. Therefore, the reliability of the GA model developed in this study in optimisation of the operational characteristics of TRSs has been validated.

ACKNOWLEDGMENTS

Mrs Jingjing Xue would like to thank China Scholarship Council (CSC) and Cardiff University for supporting this work.

REFERENCES

[1] Y. Wang *et al.*, "A global map of emission clumps for future monitoring of fossil fuel CO2 emissions from space," *Earth Syst. Sci. Data Discuss.,* vol. 2018, pp. 1-25, 2018, doi: 10.5194/essd-2018-131.

[2] S. M. Nazir, J. H. Cloete, S. Cloete, and S. Amini, "Efficient hydrogen production with CO2 capture using gas switching reforming," *Energy,* vol. 185, pp. 372-385, 2019, doi: https://doi.org/10.1016/j.energy.2019.07.072.

[3] M. Lewis *et al.*, "Power variability of tidal-stream energy and implications for electricity supply," *Energy,* vol. 183, pp. 1061-1074, 2019, doi: https://doi.org/10.1016/j.energy.2019.06.181.

[4] World Energy Council, "World Energy Resources Marine Energy," 2016. [Online]. Available: https://www.worldenergy.org/wp-content/uploads/2017/03/WEResources_Marine_2016.pdf

[5] BBC Wales, "Swansea tidal lagoon: The environmental arguments," 2016. [Online]. Available: https://www.bbc.co.uk/news/uk-wales-37863807

[6] S. P. Neill, M. R. Hashemi, and M. J. Lewis, "Optimal phasing of the European tidal stream resource using the greedy algorithm with penalty function," *Energy,* vol. 73, pp. 997-1006, 2014, doi: https://doi.org/10.1016/j.energy.2014.07.002.

[7] M. J. Lewis, A. Angeloudis, P. E. Robins, P. S. Evans, and S. P. Neill, "Influence of storm surge on tidal range energy," *Energy,* vol. 122, pp. 25-36, 2017, doi: https://doi.org/10.1016/j.energy.2017.01.068.

[8] S. P. Neill *et al.*, "Tidal range energy resource and optimization – Past perspectives and future challenges," *Renewable Energy,* pp. 763-778, 2018, doi: https://doi.org/10.1016/j.renene.2018.05.007.

[9] S. Waters and G. Aggidis, "A world first: swansea bay tidal lagoon in review," *Renewable and Sustainable Energy Reviews,* vol. 56, pp. 916-921, 2016, doi: 10.1016/j.rser.2015.12.011.

[10] Renewable Energy Focus, "Green light for world's first tidal lagoon," 2015. [Online]. Available: http://www.renewableenergyfocus.com/view/42607/green-light-for-worlds-first-tidal-lagoon/

[11] C. Hendry, "The role of tidal lagoons," 2016. [Online]. Available: https://hendryreview.files.wordpress.com/2016/08/hendry-review-final-report-english-version.pdf

[12] BBC, "David Cameron's enthusiasm for Swansea tidal lagoon 'reducing'," 2016. [Online]. Available: https://www.bbc.co.uk/news/uk-wales-politics-35306084

[13] BBC, "£1.3bn Swansea Bay tidal lagoon project thrown out," 2018. [Online]. Available: https://www.bbc.co.uk/news/uk-wales-south-west-wales-44589083

[14] D. Prandle, "Simple theory for designing tidal power schemes," *Water Resources,* vol. 7, pp. 21-27, 1984, doi: 10.1016/0309-1708(84)90026-5.

[15] I. Fairley, R. Ahmadian, R. A. Falconer, M. R. Willis, and I. Masters, "The effects of a Severn Barrage on wave conditions in the Bristol Channel," *Renewable Energy,* vol. 68, pp. 428-442, 2014, doi: 10.1016/j.renene.2014.02.023.

[16] R. Ahmadian, R. A. Falconer, and B. Bockelmann-Evans, "Comparison of hydro-environmental impacts for ebb-only and two-way generation for a Severn Barrage," *Computers & Geosciences,* vol. 71, pp. 11-19, 2014, doi: 10.1016/j.cageo.2014.05.006.

[17] J. Xia, R. A. Falconer, and B. Lin, "Impact of different operating modes for a Severn Barrage on the tidal power and flood inundation in the Severn Estuary, UK," *Applied Energy,* vol. 87, no. 7, pp. 2374-2391, 2010, doi: 10.1016/j.apenergy.2009.11.024.

[18] N. Čož, R. Ahmadian, and R. A. Falconer, "Implementation of a full momentum conservative approach in modelling flow through tidal structures," *Water,* vol. 11, no. 9, p. 1917, 2019. [Online]. Available: https://www.mdpi.com/2073-4441/11/9/1917.

[19] R. Ahmadian, J. Xue, R. A. Falconer, and N. Hanousek, "Optimisation of tidal range schemes," *The 12th European Wave and Tidal Energy Conference,* no. ISSN 2309-1983, p. 1059, 2017.

[20] N. Yates and B. Tatlock, "Optimising Tidal Lagoons," *The European Wave and Tidal Energy Conference,* 2017.

[21] A. Angeloudis, S. C. Kramer, A. Avdis, and M. D. Piggott, "Optimising tidal range power plant operation," *Applied Energy,* vol. 212, pp. 680-690, 2018, doi: 10.1016/j.apenergy.2017.12.052.

[22] J. Xue, R. Ahmadian, and R. A. Falconer, "Optimising the operation of tidal range schemes," *Energies,* vol. 12, no. 15, p. 2870, 2019. [Online]. Available: https://www.mdpi.com/1996-1073/12/15/2870.

[23] A. P. Alves da Silva and P. J. Abrao, "Applications of evolutionary computation in electric power systems," *Proceedings of the 2002 Congress on Evolutionary Computation,* pp. 1057-1062, 2002, doi: 10.1109/cec.2002.1004389.

[24] B. Pavez-Lazo and J. Soto-Cartes, "A deterministic annular crossover genetic algorithm optimisation for the unit commitment problem," *Expert Systems with Applications,* vol. 38, no. 6, pp. 6523-6529, 2011, doi: https://doi.org/10.1016/j.eswa.2010.11.089.

[25] P. Sullivan and P. McCombie, "Optimisation of tidal power arrays using a genetic algorithm," *Proceedings of the Institution of Civil Engineers,* vol. 166, pp. 19-28, 2013, doi: 10.1680/ener.12.00011.

[26] B. F. M. Child and V. Venugopal, "Optimal configurations of wave energy device arrays," *Ocean Engineering,* vol. 37, no. 16, pp. 1402-1417, 2010, doi: https://doi.org/10.1016/j.oceaneng.2010.06.010.

[27] E. Kontoleontos and S. Weissenberger, "Annual energy production maximization for tidal power plants with evolutionary algorithms," *International Journal of Fluid Machinery and Systems,* vol. 10, no. 3, pp. 264-273, 2017, doi: 10.5293/IJFMS.2017.10.3.264.

[28] P. B. Leite Neto, O. R. Saavedra, and L. A. Souza Ribeiro, "Optimization of electricity generation of a tidal power plant with reservoir constraints," *Renewable Energy,* vol. 81, pp. 11-20, 2015, doi: 10.1016/j.renene.2015.03.011.

[29] J. R. Koza, "Genetic programming as a means for programming computers by natural selection," *Statistics and Computing,* vol. 4, no. 2, pp. 87-112, 1994, doi: 10.1007/bf00175355.

[30] J. H. Holland, "Adaptation in natural and artificial systems," 1975.

[31] S. R. Ladd, "Genetic Algorithms in C++," 1995.

[32] M. B. Nia and Y. Alipouri, "Speeding up the genetic algorithm convergence using sequential mutation and circular gene methods," *The 9th International Conference on Intelligent Systems Design and Applications,* pp. 31-36, 2009, doi: 10.1109/ISDA.2009.140.

[33] L. B. Booker, "Recombination distributions for genetic algorithms," *Foundations of Genetic Algorithms,* vol. 2, pp. 29-44, 1993, doi: https://doi.org/10.1016/B978-0-08-094832-4.50008-8.

[34] A. Guven, "Linear genetic programming for time-series modelling of daily flow rate," *Journal of Earth System Science,* vol. 118, no. 2, pp. 137-146, 2009, doi: 10.1007/s12040-009-0022-9.

[35] R. Dulbecco and M. Vogt, "Evidence for a ring structure of polyoma virus DNA," *Proceedings of the National Academy of Sciences of the United States of America,* vol. 50, no. 2, pp. 236-243, 1963. [Online]. Available: http://www.ncbi.nlm.nih.gov/pmc/articles/PMC221161/.

[36] R. Weil and J. Vinograd, "The cyclic helix and cyclic coil forms of polyoma viral DNA," *Proceedings of the National Academy of Sciences,* vol. 50, no. 4, p. 730, 1963. [Online]. Available: http://www.pnas.org/content/50/4/730.abstract.
[37] E. Zitzler, K. Deb, and L. Thiele, "Comparison of multiobjective evolutionary algorithms: empirical results," *Evolutionary Computation,* vol. 8, no. 2, pp. 173-195, 2000, doi: 10.1162/106365600568202.
[38] J. L. R. Filho, P. C. Treleaven, and C. Alippi, "Genetic-algorithm programming environments," *Computer,* vol. 27, no. 6, pp. 28-43, 1994, doi: 10.1109/2.294850.
[39] G. Chennupati, R. M. A. Azad, and C. Ryan, "Automatic evolution of parallel recursive programs," *Genetic Programming,* pp. 167-178, 2015, doi: 10.1007/978-3-319-16501-1_14.
[40] D. E. Goldberg, "Genetic algorithms in search, optimization and machine learning," p. 372, 1989.
[41] S. Petley and G. Aggidis, "Swansea Bay tidal lagoon annual energy estimation," *Ocean Engineering,* vol. 111, pp. 348-357, 2016, doi: 10.1016/j.oceaneng.2015.11.022.
[42] "Swansea Bay Tidal Lagoon," 2018. [Online]. Available: http://www.tidallagoonpower.com/projects/swansea-bay/
[43] G. Rajgor, "Time for tidal lagoons?," *Renewable Energy Focus,* vol. 17, no. 5, pp. 202-204, 2016, doi: 10.1016/j.ref.2016.08.010.
[44] Support The Guardian, "Government rejects plan for £1.3bn tidal lagoon in Swansea," 2018. [Online]. Available: https://www.theguardian.com/business/2018/jun/25/government-rejects-plan-for-tidal-lagoon-in-swansea
[45] A. Angeloudis, R. Ahmadian, R. A. Falconer, and B. Bockelmann-Evans, "Numerical model simulations for optimisation of tidal lagoon schemes," *Applied Energy,* vol. 165, pp. 522-536, 2016, doi: 10.1016/j.apenergy.2015.12.079.
[46] S. Bray, R. Ahmadian, and R. A. Falconer, "Impact of representation of hydraulic structures in modelling a Severn barrage," *Computers & Geosciences,* vol. 89, pp. 96-106, 2016, doi: 10.1016/j.cageo.2016.01.010.
[47] G.Aggidis and O.Feather, "Tidal range turbines and generation on the Solway Firth," *Renewable Energy,* vol. 43, pp. 9-17, 2012, doi: https://doi.org/10.1016/j.renene.2011.11.045.
[48] R. Ahmadian, C. Morris, and R. A. Falconer, "Hydro-environmental modelling of off-shore and coastally attached impoundments off the north wales coast," *Proceedings of the 1st European IAHR Congress,* 2010. [Online]. Available: http://orca.cf.ac.uk/id/eprint/7601.
[49] R. Ahmadian, R. A. Falconer, and B. Bockelmann-Evans, "Far-field modelling of the hydro-environmental impact of tidal stream turbines," *Renewable Energy,* vol. 38, no. 1, pp. 107-116, 2012, doi: 10.1016/j.renene.2011.07.005.
[50] J. Xia, R. A. Falconer, B. Lin, and G. Tan, "Estimation of annual energy output from a tidal barrage using two different methods," *Applied Energy,* vol. 93, pp. 327-336, 2012, doi: 10.1016/j.apenergy.2011.12.049.
[51] R. A. Falconer, "Flow and water-quality modelling in coastal and inland water," *Journal of Hydraulic Research,* vol. 30, no. 4, pp. pp. 437-452, 1992, doi: 10.1080/00221689209498893
[52] "DiGSBS250K [SHAPE geospatial data], scale 1:250000, tiles: GB, updated: 6 September 2011, BGS, using: EDINA Geology Digimap Service, <http://digimap.edina.ac.uk>, downloaded: 2017," ed.
[53] Swansea Bay Tidal Lagoon, "Dredging Work," vol. 2. [Online]. Available: http://www.tidallagoonpower.com/wp-content/uploads/2017/05/DCO-Application-2.4.40-dredging-works.pdf
[54] D. Whitley, "Genetic algorithm and neural network," 1995.
[55] K. Zhu and Z. Liu, "Population diversity in permutation based genetic algorithm," pp. 537-547, 2004, doi: 10.1007/978-3-540-30115-8_49.